Rotational Spectra of the Less Common Isotopomers, Electric Dipole Moment and the Double Minimum Inversion Potential of $H_2O\cdots HCl$

Z. Kisiel* and B. A. Pietrewicz

Institute of Physics, Polish Academy of Sciences, Al. Lotników 32/46, 02-668 Warszawa, Poland

P. W. Fowler, A. C. Legon, and E. Steiner

School of Chemistry, University of Exeter, Stocker Rd., Exeter EX4 4QD, United Kingdom

Received: March 28, 2000; In Final Form: May 16, 2000

Rotational spectra of 14 different isotopomers of the hydrogen-bonded dimer $H_2O\cdots HCl$ have been measured. On application of a method of analysis designed to minimize the effect of vibration−rotation contributions to the ground state geometry, it was found that the experimental rotational constants imply a nonplanar geometry with $R_0(OCl) = 3.2273(3)$ Å, and an out-of-plane bend angle of the water subunit $\phi_0 = 34.7(4)°$. This angle is consistent with results of ab initio calculations which, at the BSSE corrected, aug-cc-pVDZ/MP2 level, give $\phi = 46°$ for the equilibrium configuration and $\phi = 35.2°$ for the ground state. The electric dipole moment of $H_2O\cdots HCl$, $\mu = 3.437(4)$ D, was determined from Stark effect measurements and, after allowance for the zero-point inversion motion of the water subunit, leads to dipole moment enhancement on complexation $\Delta\mu = 0.81$ D. Theoretical analysis of contributions to the chlorine nuclear quadrupole splitting constant χ_{aa} for $H_2O\cdots HCl$ shows that most of the reduction relative to its value in free HCl is accounted for by the response of the complexed HCl to the nonuniform field of the nearby H_2O subunit. The remaining difference, ascribed to motional averaging, implies an operationally defined angle of oscillation for the HCl moiety of 10°−12°.

Introduction

In the early investigations of hydrogen-bonded complexes in the gas phase, species of the type $H_2O\cdots HX$, involving a water molecule as the proton acceptor and a hydrogen halide HX as the proton donor, featured prominently for several reasons. First, simple five-atom complexes provide an appropriate meeting point for experiment and theory. Second, the interaction of water and hydrogen halide molecules presumably forms the initial step in a chemically familiar phenomenon, namely the nucleation of droplets to produce the mist familiar when hydrogen halide gases fume in moist air. The third reason for interest in complexes $H_2O\cdots HX$ lies in their angular geometry. According to some empirical rules for predicting the angular geometries of hydrogen-bonded complexes, first enunciated explicitly in 1982, ref 1, but implied in some earlier publications,[2,3] the *equilibrium* geometry of $H_2O\cdots HX$ should involve a pyramidal arrangement at O, given that the rules require HX to lie along the axis of a nonbonding electron pair on O.

The first $H_2O\cdots HX$ complex to be investigated spectroscopically in the gas phase was $H_2O\cdots HF$.[4−6] The strength of the $O\cdots H-F$ bond is sufficient[7,8] to allow the observation of this species in equilibrium gas mixtures of H_2O and HF. Moreover, investigations of its rotational and vibrational spectra were thereby possible at temperatures high enough to yield significant populations of vibrationally excited states of the intermolecular bending and stretching modes. Hence, vibrational satellites associated with such states were observed in the rotational spectrum when detected with a conventional Stark modulation microwave spectrometer.[4,5,9] A detailed analysis of the variation of rotational constants and the electric dipole moment of the complex with the vibrational quantum number $v_{\beta(o)}$, where the subscript β(o) indicates the low frequency, out-of-plane intermolecular bending mode, allowed a quantitative determination[5] of the one-dimensional potential energy function $V(\phi)$ associated with the out-of-plane angle ϕ defined in Figure 1. It was found that $V(\phi)$ is of the double-minimum type, with $\phi_e = \pm 46(8)°$ and with a potential energy barrier of only 126 cm^{-1} at the planar ($\phi = 0$) geometry. The significance of this result was that it showed the equilibrium configuration at O to be pyramidal, with the angle ϕ_e close to the value of half the tetrahedral angle required by the empirical rules. On the other hand, the zero-point energy level is very close to the top of the potential energy barrier.[5] Evidently, in the zero-point state, $H_2O\cdots HF$ is *effectively planar*, in the sense that the vibrational wave functions may be classified according to the C_{2v}, rather than the C_s, point group. If only the spectroscopic constants for the vibrational ground state were available it would be much more

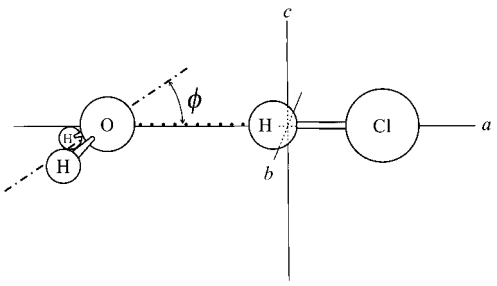

Figure 1. Geometry of the hydrogen-bonded dimer $H_2O\cdots HCl$, which is drawn to scale for the ground vibrational state. The positions of the three inertial axes are indicated.

* Corresponding author. E-mail: kisiel@ifpan.edu.pl. Fax: +48-22-8430926.

10.1021/jp001156o CCC: $19.00
Published on Web 07/11/2000

difficult to distinguish between a strictly planar and an effectively planar geometry.

The hydrogen bond in the next member of the $H_2O\cdots HX$ series (X = Cl) is sufficiently weak that the complex $H_2O\cdots HCl$ has not been observed in equilibrium gas mixtures. When the temperature is low enough to give an equilibrium constant of sufficient magnitude, the vapor pressure above the condensed phase is negligible. Accordingly, $H_2O\cdots HCl$ was first observed in the gas phase by a technique employing supersonic expansion. A preliminary report of the ground-state rotational spectra of the two isotopomers $H_2{}^{16}O\cdots H^{35}Cl$ and $H_2{}^{16}O\cdots H^{37}Cl$, as observed by the pulsed-nozzle, Fourier transform technique, has already been published.[10] Because of the low effective temperature of the expanded gas mixture, only ground-state rotational transitions were observed and, consequently, it was not possible to decide whether $H_2O\cdots HCl$ is strictly planar or effectively planar (in the sense defined earlier), although on chemical grounds it seemed probable that the equilibrium geometry is nonplanar and the potential energy barrier at $\phi = 0$ is very low.

In this paper, we present a detailed analysis of the ground-state rotational spectra of 14 isotopomers of the $H_2O\cdots HCl$ complex, thereby consolidating the preliminary report in this series. By combining the extensive set of spectroscopic constants so obtained with the results of high-level ab initio calculations and our experience with $H_2O\cdots HF$, it is possible to conclude that $H_2O\cdots HCl$ has a pyramidal configuration at O in the equilibrium conformation but that in the zero-point state there is a very low barrier to the planar form. The dimer $H_2O\cdots HCl$ is, like $H_2O\cdots HF$, effectively planar according to the symmetry classification of the wave function, although it is found below that the ground-state geometry shows marked nonplanarity. The electric dipole moment μ of $H_2O\cdots HCl$ was measured by means of the Stark effect and the experimental results and ab initio calculations have been combined to reach an understanding of the differences in the dipole moment and in the nuclear quadrupole splitting constant in the complex from the values derivable from free monomers.

Experimental Details

The complex was observed in supersonic expansion with the cavity Fourier transform microwave (FTMW) spectrometer in Warsaw,[11,12] which is a coaxial waveguide version of the well-known Balle−Flygare design.[13] Initially, the complex was obtained, as in the original investigation,[10] by mixing gaseous HCl and H_2O with Ar carrier gas and also by flowing an HCl/Ar mixture over a sample of liquid water. It was found, however, that a more convenient and reproducible procedure was to simply flow Ar carrier gas over a sample of concentrated aqueous hydrochloric acid. The acid sample was kept at room temperature, and only a small proportion of the Ar gas flow was passed over the acid, the remainder being directed through a bypass tube joining the sample flow at a T-joint just ahead of the expansion nozzle. Deuterated isotopomers were obtained from concentrated acid prepared by condensing an appropriate amount of gaseous HCl into a sample of D_2O, and similarly, the ^{18}O isotopomers were observed using acid prepared from HCl and $H_2{}^{18}O$. The gaseous mixture, at a backing pressure of ca. 1.1 atm, was expanded through a modified General-Valve Corp. Series 9 valve, in a direction perpendicular to the axis of the microwave cavity. This experimental method enabled simultaneous observation of related higher multimers, $(H_2O\cdots HCl)\cdots Ar$[14] and $(H_2O)_2HCl$.[15]

Stark effect measurements were made with a cell consisting of two 28 × 28 cm parallel plate aluminum electrodes, spaced 27 cm apart. The electrode design was optimized through numerical electric field calculations and, as a result, the two flat plates were augmented with several side and corner plates, which produced a considerable improvement in uniformity of the electric field. The electrodes were initially separated by dielectric rods but, since all insulating materials were found to collect some electric charge and degrade field homogeneity, the rods were removed from the design. One electrode was suspended from the top of the chamber, and the second was placed on legs resting on the chamber bottom. Appropriate mechanical design ensured reproducible and parallel electrode placement. Further details will be published elsewhere. The electric field was produced by applying symmetrically opposed voltages to the two electrodes, and fields of up to 185 V/cm were employed in this investigation. Calibrations were carried out by using CH_3I, $\mu = 1.6406(4)$ D,[16] and CH_3CN, $\mu = 3.921\,97(13)$ D.[17] Only the $\Delta M = 0$ Stark components were measured, by orienting the L-type aerials in the microwave resonator of the FTMW spectrometer[12] parallel to the direction of the applied electric field. The $\Delta M = \pm 1$ components are also accessible with the perpendicular aerial/field orientation.

Rotational Spectrum

Only four a-type rotational transitions, $1_{01} \leftarrow 0_{00}$, $2_{02} \leftarrow 1_{01}$, $2_{12} \leftarrow 1_{11}$, and $2_{11} \leftarrow 1_{10}$, can be observed in the frequency region of the spectrometer. For $H_2O\cdots H^{35}Cl$, the two $J = 2 \leftarrow 1$ $K_{-1} = 1$ transitions are found to be more intense than the $K_{-1} = 0$ transition. This implies both a relatively small population difference due to rotational cooling and the existence of nuclear spin statistical weights expected for a planar or effectively planar complex, which are 1:3 and 2:1 for $K_{-1} =$ 0:1 for $H_2O\cdots HCl$, and $D_2O\cdots HCl$, respectively. The two $K_{-1} = 1$ transitions originate from energy levels, which are estimated to be 14 cm^{-1} above the $K_{-1} = 0$ levels, and would normally be depopulated at the 1 K rotational temperature of the supersonic expansion. These transitions are observed, however, through the phenomenon of condensation of excited states of a given spin parity to the lowest level of the same spin parity.[18] For complexes of H_2O with hydrogen chloride, the $K_{-1} = 0$ levels are the lowest levels carrying the antisymmetric spin function and the $K_{-1} = 1$ levels are the lowest levels with the symmetric spin function, whereas the reverse is true for the D_2O isotopomers. The parity distinction disappears in $HDO\cdots HCl$, and in this case He carrier gas was used to increase the effective temperature so that the very weak $K_{-1} = 1$ lines could be observed. Each rotational transition is a multiplet arising from the presence of the chlorine nucleus, which allows the chlorine nuclear quadrupole splitting constant in the complex to be measured. The determinable spectroscopic constants are listed in Tables 1−3, for all isotopomers arising from deuteration of $H_2{}^{16}O\cdots H^{35}Cl$, deuteration of $H_2{}^{16}O\cdots H^{37}Cl$, and the two observed $H_2{}^{18}O$ containing isotopomers, respectively. In addition, analysis of additional splitting introduced by the deuterium nucleus in $H_2{}^{16}O\cdots D^{35}Cl$ allowed the quadrupole constant for this nucleus, $\chi_{aa}(D) = 0.0147(10)$ MHz, to be determined. Even in $H_2{}^{16}O\cdots H^{35}Cl$ the individual components of the chlorine hyperfine structure were observed to exhibit varying degrees of further splitting, arising from the presence of the three protons. Some attempt to resolve and to fit such structure was made, whereupon it was found that physically meaningful constants are obtained only on inclusion of all four nonzero spin nuclei in the model. The dominant small constants are found to be the spin−spin and spin-rotation constants associated with the two water hydrogen atoms, H_a and H_b. On fixing the smaller spin−spin constants between the HCl and H_2O hydrogens at

TABLE 1: Spectroscopic Constants of $H_2{}^{16}O\cdots H^{35}Cl$ and of All Isotopomers that Can Be Obtained by Its Deuteration

		$H_2{}^{16}O\cdots H^{35}Cl$	$H_2{}^{16}O\cdots D^{35}Cl$	$HD^{16}O\cdots H^{35}Cl$	$HD^{16}O\cdots D^{35}Cl$	$D_2{}^{16}O\cdots H^{35}Cl$	$D_2{}^{16}O\cdots D^{35}Cl$
B	(MHz)	3931.2969(11)[a]	3936.4945(14)	3737.3681(15)	3743.3401(16)	3566.6757(12)	3573.1312(19)
C	(MHz)	3891.5897(11)	3897.0580(14)	3685.1472(15)	3691.3001(16)	3505.3014(12)	3511.9903(19)
$B+C$	(MHz)	7822.8866(16)	7833.5525(20)	7422.5153(21)	7434.6402(23)	7071.9771(17)	7085.1215(27)
$B-C$	(MHz)	39.7072(16)	39.4365(20)	52.2209(21)	52.0400(23)	61.3743(17)	61.1409(27)
Δ_J	(MHz)	0.01448(14)	0.01346(18)	0.01307(18)	0.01305(16)	0.01182(15)	0.01183(23)
Δ_{JK}	(MHz)	1.12071(35)	0.98003(47)	0.64406(44)	0.54905(64)	0.90213(36)	0.81565(58)
χ_{aa}	(MHz)	−53.4137(23)	−54.7722(28)	−53.3749(24)	−54.6925(30)	−53.3807(23)	−54.6667(24)
χ_{bb}	(MHz)	26.3792(31)	27.0400(40)	26.3542(44)		26.3932(39)	27.0252(46)
χ_{cc}	(MHz)	27.0345(31)	27.7322(40)	27.0207(44)		26.9875(39)	27.6416(46)
η[b]		0.01227(8)	0.01264(10)	0.01249(12)		0.01113(10)	0.01127(12)
N lines[c]		4,24	4,20	4,21	4,11	4,22	4,20
σ[d]	(kHz)	2.5	3.0	3.1	2.3	2.6	3.9

[a] The quantities in parentheses are standard errors in units of the least significant digit of the value. [b] η is the nuclear quadrupole symmetry parameter defined by $\eta = (\chi_{bb} - \chi_{cc})/\chi_{aa}$. [c] The number of measured rotational, and hyperfine transitions, respectively. [d] The total deviation of fit.

TABLE 2: Spectroscopic Constants of $H_2{}^{16}O\cdots H^{37}Cl$ and of All Isotopomers that Can Be Obtained by Its Deuteration

		$H_2{}^{16}O\cdots H^{37}Cl$	$H_2{}^{16}O\cdots D^{37}Cl$	$HD^{16}O\cdots H^{37}Cl$	$HD^{16}O\cdots D^{37}Cl$	$D_2{}^{16}O\cdots H^{37}Cl$	$D_2{}^{16}O\cdots D^{37}Cl$
B	(MHz)	3859.2996(11)	3863.9645(15)			3497.0884(11)	3503.2142(17)
C	(MHz)	3821.0251(11)	3825.9572(15)			3438.0605(11)	3444.4196(17)
$B+C$	(MHz)	7680.3247(16)	7689.9217(21)	7282.9996(30)	7294.2764(24)	6935.1489(16)	6947.6338(24)
$B-C$	(MHz)	38.2745(16)	38.0073(21)			59.0279(16)	58.7946(24)
Δ_J	(MHz)	0.01408(14)	0.01278(19)	0.01291(21)	0.01256(16)	0.01131(14)	0.01134(21)
Δ_{JK}	(MHz)	1.07231(32)	0.93924(54)			0.86090(36)	0.77811(58)
χ_{aa}	(MHz)	−42.0967(23)	−43.1739(29)	−42.0691(41)	−43.1065(41)	−42.0591(28)	−43.0991(29)
χ_{bb}	(MHz)	20.7806(31)	21.3062(40)			20.8090(40)	21.3038(47)
χ_{cc}	(MHz)	21.3162(31)	21.8678(40)			21.2501(40)	21.7954(47)
η		0.01272(10)	0.01301(13)			0.01049(13)	0.01141(15)
N		4,26	4,19	2,8	2,8	4,20	4,18
σ	(kHz)	2.7	3.1	3.2	2.5	2.3	3.4

TABLE 3: Spectroscopic Constants of $H_2{}^{18}O\cdots H^{35}Cl$ and $H_2{}^{18}O\cdots H^{37}Cl$

		$H_2{}^{18}O\cdots H^{35}Cl$	$H_2{}^{18}O\cdots H^{37}Cl$
B	(MHz)	3686.5033(15)	3614.3822(13)
C	(MHz)	3651.6208(15)	3580.8447(13)
$B+C$	(MHz)	7338.1241(21)	7195.2269(18)
$B-C$	(MHz)	34.8825(21)	33.5375(18)
Δ_J	(MHz)	0.01282(19)	0.01230(16)
Δ_{JK}	(MHz)	0.98473(44)	0.93948(37)
χ_{aa}	(MHz)	−53.4129(23)	−42.1002(23)
χ_{bb}	(MHz)	26.3650(26)	20.7813(26)
χ_{cc}	(MHz)	27.0479(26)	21.3189(26)
η		0.01278(7)	0.01277(9)
N		4,26	4,26
σ	(kHz)	3.4	2.9

values calculated as in ref 19, we determine spin−spin constants, $D_{aa}(H_aH_b) = 36(9)$ kHz, $D_{bb}-D_{cc}(H_aH_b) = -104(18)$ kHz, and the spin-rotation constants $M_{aa}(H_a) = M_{aa}(H_b) = -29(3)$ kHz, which are close to those in the free water molecule, $D_{aa}(H_aH_b) = 33.8$ kHz, $D_{bb}-D_{cc}(H_aH_b) = -102$ kHz (calculated), and $M_{aa}(H_a) = M_{aa}(H_b) = -30.68(30)$ kHz[20] (obtained from experimental values by transforming the axes).

A useful starting point for further interpretation of the experimental data is provided by application of several simple models, as summarized in Table 4. The structural parameters are obtained from the planar model employed in the original investigation.[10] The nuclear quadrupole coupling constant $\chi_{aa}(Cl)$ was used to derive the large-amplitude oscillation angle of the HCl moiety from the operational definition introduced by Novick et al.[21] Finally, the centrifugal distortion constant D_J was used to calculate the pseudo-diatomic stretching constant, f_σ, by means of the enhanced formulas compensating for asymmetry.[22,23]

Intercomparisons between the isotopomers reveal that the planar geometry gives consistent results for heavy atom substitution, but there are two different effects for deuterium substitution. Complexation with DCl leads to apparent shortening of the R_0(OCl) distance by 0.0025 Å, which is rationalizable in terms of the well-known Ubbelohde effect.[24] It is more difficult to rationalize changes in R_0(OCl) on $H_2O \rightarrow HDO \rightarrow D_2O$ substitution. These provide evidence of a nonplanar ground-state geometry, which is explored in more detail below. The oscillation angle θ_{av} shows very little variation within the HCl family or within the DCl family of isotopomers, whereas there is an appreciable difference between the two families. θ_{av} values for the DCl isotopomers are systematically smaller than those for the HCl equivalents, in line with anticipated decrease in the oscillation amplitude resulting from the increase in the reduced mass for the motion and the stronger O···DCl hydrogen bond. The isotopic behavior of f_σ is clear for the H_2O isotopomers, and consistent with the Ubbelohde effect, in that the values for DCl are greater than those for HCl, but this pattern seems to disappear on deuteration of the H_2O subunit.

Inspection of the remaining constants in Tables 1−3 reveals that while the centrifugal distortion constant D_J decreases with mass of the complex, the constant D_{JK} shows zigzag behavior with deuteration of the water subunit. For example, for the $H^{35}Cl$ series D_{JK} is 1.1207(4), 0.6441(4), and 0.9021(4) MHz for $H_2{}^{16}O$, $HD^{16}O$, and $D_2{}^{16}O$, respectively. Behavior of this type is often indicative of an isotope-specific perturbation and has for this reason been tested against a simple, planar force-field model, constructed along the lines used previously for $H_2O\cdots HF$.[25] On using only two independent force constants, $f_\sigma = 12.9$ N m^{-1} and $f_\alpha = f_\theta = f_\phi = 2.16 \times 10^{-20}$ J rad^{-2}, which reproduce D_J and D_{JK} for the parent isotopomer, the corresponding values for $HD^{16}O\cdots H^{35}Cl$ and $D_2{}^{16}O\cdots H^{35}Cl$ are $D_J = 13.0$ and 11.4 kHz, respectively, and $D_{JK} = 0.715$ and 0.866 MHz, respectively. Thus the zigzag behavior is reproducible and arises from the isotopic behavior of the linear combination

TABLE 4: Parameters for the Measured Isotopomers of the Dimer between H_2O and HCl Derived on the Basis of the Planar Geometry and Two Commonly Used Simple Models

		$H_2{}^{16}O\cdots H^{35}Cl$	$H_2{}^{16}O\cdots H^{37}Cl$	$HD^{16}O\cdots H^{35}Cl$	$HD^{16}O\cdots H^{37}Cl$	$D_2{}^{16}O\cdots H^{35}Cl$	$D_2{}^{16}O\cdots H^{37}Cl$	$H_2{}^{18}O\cdots H^{35}Cl$	$H_2{}^{18}O\cdots H^{37}Cl$
R_0(OCl)	(Å)	3.2151	3.2149	3.2095	3.2093	3.2050	3.2049	3.2156	3.2154
R_{cm}	(Å)	3.2450	3.2468	3.2673	3.2691	3.2875	3.2893	3.2389	3.2406
$\theta_{av}{}^a$	(deg)	21.977	21.979	22.009	22.007	22.004	22.018	21.978	21.975
$f_\sigma{}^b$	(N m^{-1})	12.72	12.61	12.45	[12.13]	12.28	12.34	12.73	12.75
		$H_2{}^{16}O\cdots D^{35}Cl$	$H_2{}^{16}O\cdots D^{37}Cl$	$HD^{16}O\cdots D^{35}Cl$	$HD^{16}O\cdots D^{37}Cl$	$D_2{}^{16}O\cdots D^{35}Cl$	$D_2{}^{16}O\cdots D^{37}Cl$		
R_0 (OCl)	(Å)	3.2125	3.2123	3.2066	3.2064	3.2018	3.2017		
R_{cm}	(Å)	3.2084	3.2119	3.2305	3.2339	3.2503	3.2538		
θ_{av}	(deg)	20.692	20.687	20.760	20.760	20.782	20.768		
f_σ	(N m^{-1})	13.70	13.89	12.50	[12.49]	12.32	12.35		

[a] θ_{av} is defined operationally by $\chi_{complex} = (1/2)\chi_{HCl}(3\cos^2\theta_{av} - 1)$, ref 21. [b] Calculated from D_J, ref 22.

of the centrifugal τ components which constitutes D_{JK}, and is due to the much increased values of τ_{aabb} and τ_{aacc} in the HDO containing isotopomer over those in the two symmetric ones. The success of the simple force field calculation arises from the rather limited vibrational mode dependence of the two centrifugal distortion constants. D_J depends primarily on the intermolecular stretching mode ν_σ, which forms the basis for the pseudo-diatomic approximation, whereas, in a planar $H_2O\cdots HX$ type complex, D_{JK} is found to depend primarily on the lowest frequency in-plane-bending mode $\nu_{\beta(i)}$.

Double Minimum Potential

For the related dimer $H_2O\cdots HF$, the shape of this section of the potential energy function was derived entirely on the basis of experimental data.[5] This was made feasible by observation of the dimer in vibrationally excited states. For $H_2O\cdots HCl$ this is not possible since the FTMW technique only delivers information about the vibrational ground state. Several of the observables do, however, have some sensitivity to the shape of the potential, so that they can be compared with appropriate predictions once the potential surface is available by other means. It is possible, therefore, to determine the double minimum potential surface by ab initio calculations and, by taking $H_2O\cdots HF$ as a benchmark, to compare this with the spectroscopic results for $H_2O\cdots HCl$.

The calculations were carried out with GAMESS,[26] at the aug-cc-pVDZ/MP2 level,[27] which was previously shown to deliver accurate results for intermolecular complexes containing water.[28,29] The energy values were determined by carrying out full optimizations for fixed values of the out-of-plane bending coordinate ϕ. The energies were then corrected for the basis set superposition error (BSSE), using the counterpoise correction method of Boys and Bernardi,[30] as built into GAMESS. The resulting potential is shown in Figure 2. The potential has minima at $\phi_{min} = 45.7°$ and the central barrier, V_0, is 80 cm^{-1}. The dissociation energy, D_e, is calculated to be 22.2 kJ mol^{-1}. These values are consistent with previous theoretical equilibrium geometries.[31,32] The same level of calculation gives $\phi_{min} = 48.5°$, $V_0 = 146$ cm^{-1}, and $D_e = 33.6$ kJ mol^{-1} for $H_2O\cdots HF$, which is in agreement with the experimentally determined quantities $\phi_{min} = 46(8)°$ and $V_0 = 126(70)$ cm^{-1} from ref 5, and $D_e = 30$ kJ mol^{-1}, ref 6.

To examine the consistency of the theoretical potential with the spectroscopic variables, we need to be able to evaluate the positions of the energy levels and the appropriate expectation values. We choose to do this by approximating the ab initio energy with the quartic−quadratic potential

$$V = a\phi^2 + b\phi^4 \qquad (1)$$

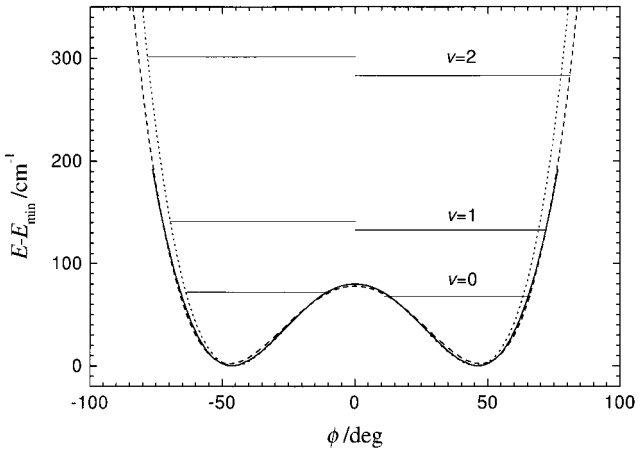

Figure 2. Ab initio double minimum potential along the out-of-plane bending coordinate for $H_2O\cdots HCl$, and its approximation by means of the quartic-quadratic potential defined by the barrier height and ϕ_{min} (dotted line) and fitted numerically (dashed line). The positions of the vibrational energy levels are indicated.

which has seen much application in spectroscopy, and the properties of which are very well-known.[33] The reduced form of the quartic−quadratic potential

$$V = A(z^2 + Bz^4) \qquad (2)$$

is particularly convenient, since it is possible to use existing tabulations of eigenvalues and expectation values,[34] and the necessary conversion relations between parameters of eq 1 and eq 2 have been given in ref 5. We approximated the ab initio potential in two ways. The parameters of the potential function were first calculated from the extrema, namely the values of ϕ_{min} and V_0. The second choice was to fit the quartic−quadratic function numerically to the calculated energies. The comparison with the ab initio potential shows that both quartic−quadratic functions are satisfactory, although the fitted function is preferred. The parameters of the corresponding reduced potential are $A = 50.16$ cm^{-1}, $B = -2.463$, and the conversion to eq 1 is possible by using $z = 1.343\phi$.[5] The positions of the energy levels for the two quartic−quadratic potentials marked in Figure 2 provide a measure of their sensitivity to the particular choice of the potential function. In both cases the ground-state level lies within 10 cm^{-1} from the top of the barrier.

For a molecule subject to inversion between two symmetrically equivalent nonplanar minima, an important question concerns the geometry in the quantum states in which the molecule is actually observed. Quantum mechanical averages of odd powers of the oscillation coordinate in the quartic quadratic potential are zero, so it is not possible to determine $\langle\phi\rangle_{vv}$ directly. Fortunately, moments of inertia are not directly

TABLE 5: Comparison of the Distances R_0(OCl) (Å) for the Isotopomers of $H_2O\cdots HCl$ Derived on the Basis of Planar and of Pyramidal Geometries

	$H_2{}^{16}O\cdots H^{35}Cl$	$H_2{}^{16}O\cdots H^{37}Cl$	$HD^{16}O\cdots H^{35}Cl$	$HD^{16}O\cdots H^{37}Cl$	$D_2{}^{16}O\cdots H^{35}Cl$	$D_2{}^{16}O\cdots H^{37}Cl$	$H_2{}^{18}O\cdots H^{35}Cl$	$H_2{}^{18}O\cdots H^{37}Cl$	mean
planar, $\phi = 0°$	3.2151	−0.0002[a]	−0.0056	−0.0058	−0.0101	−0.0102	0.0005	0.0003	
nonplanar, $\phi = 35.2°$	3.2282	−0.0002	−0.0003	−0.0005	−0.0002	−0.0003	−0.0007	−0.0009	3.2280(4)
	$H_2{}^{16}O\cdots D^{35}Cl$	$H_2{}^{16}O\cdots D^{37}Cl$	$HD^{16}O\cdots D^{35}Cl$	$HD^{16}O\cdots D^{37}Cl$	$D_2{}^{16}O\cdots D^{35}Cl$	$D_2{}^{16}O\cdots D^{37}Cl$			
planar, $\phi = 0°$	3.2125	−0.0002	−0.0059	−0.0061	−0.0107	−0.0108			
nonplanar, $\phi = 35.2°$	3.2256	−0.0001	−0.0006	−0.0007	−0.0008	−0.0009			3.2253(3)

[a] The difference relative to the parent isotopomer in the HCl or the DCl series.

sensitive to ϕ, but to $\cos(\phi)$, which defines a projection close to that which is required to determine the inertial coordinates of the nonplanar hydrogen atoms. The quantum mechanical average over the wave function of the double minimum potential, $\langle\cos(\phi)\rangle_{00}$, can be obtained through expansion in terms of the vibrational coordinate since

$$\langle\cos(\phi)\rangle_{vv} = 1 - \frac{1}{2}\langle\phi^2\rangle_{vv} + \frac{1}{24}\langle\phi^4\rangle_{vv} - \ldots \qquad (3)$$

and $\langle\phi^2\rangle_{vv}$ and $\langle\phi^4\rangle_{vv}$ can be calculated from the values of $\langle z^2\rangle_{vv}$ and $\langle z^4\rangle_{vv}$ tabulated in ref 34. This allows ϕ_0 to be estimated from $\cos^{-1}\langle\cos(\phi)\rangle_{00}$, which, for the preferred quartic−quadratic potential for $H_2O\cdots HCl$, leads to $\phi_0 = 35.2°$. ϕ_0 may exhibit considerable variation with the vibrational quantum number and it is found to be critically dependent on the position of the energy level in question relative to the top of the potential barrier. There is also the possibility of some isotopic variation arising from the changes in the reduced mass for the motion,[5] although the difference in ϕ_0 between $H_2O\cdots HCl$ and $D_2O\cdots HCl$ is calculated to be well below 0.5°.

Molecular Structure

The observation of isotopomers arising from substitution of both heavy atoms in the dimer leads, with the use of Kraitchman's equation,[35] to the substitution heavy atom distance r_s(OCl) = 3.218(2) Å. Identical results are obtained irrespective of whether $H_2{}^{16}O\cdots H^{35}Cl$ or $H_2{}^{16}O\cdots H^{37}Cl$ is used as the parent isotopomer. The error is assigned according to Costain's criterion of $\delta z = 0.0015/|z|$.[36]

It is well-known that the substitution analysis suffers from sensitivity to vibrational contributions to rotational constants, and a least-squares ground state, r_0, analysis is usually preferred. In Table 5 we first explore the differences in R_0(OCl) determined for each isotopomer with the planar model, as well as with the nonplanar model with $\phi_0 = \cos^{-1}\langle\cos(\phi)\rangle_{00} = 35.2°$. The success of the nonplanar model is quite evident, although this conclusion has only been made possible by the availability of the deuterated water isotopomers of the complex. Prior to fitting the rotational constants, we note that the complex is highly prolate so that the two measured rotational constants B and C are rather similar. Since it is preferable to fit structural parameters to the moments of inertia, the values of B and C imply that $I_b + I_c$ is much larger than $I_c - I_b$, which for $H_2{}^{16}O\cdots H^{35}Cl$ is only 1.312 u Å^2. In the several hydrogen-bonded complexes for which harmonic vibration−rotation contributions to moments of inertia have been calculated,[15,37,38] their magnitude has been at the level of 0.5−1 u Å^2. It is clear, therefore, that the use of $I_c - I_b$, i.e. of independent values of I_c and I_b will be subject to considerable error. This argument is reinforced by the unknown anharmonic contributions, which may be at least comparable in magnitude to the harmonic ones. For this reason we decided to use only the linear combination $I_b + I_c$ to fit the structural parameters. In practice it is the quantity

$$(\hbar/\pi)/(B + C) = 4I_bI_c/(I_b + I_c) \cong I_b + I_c \qquad (4)$$

which was fitted, as it allows the rotational constant $(B + C)$ to be used, and for some complexes this is the only rotational constant that is available. The basis for the sensitivity of this quantity to $\langle\cos(\phi)\rangle_{00}$ becomes clear on evaluation of the contribution to it from the two water hydrogen atoms which is

$$(I_b + I_c)_H = 2m_H(2a_H{}^2 + b_H{}^2 + c_H{}^2) \cong 2m_H(2a_O{}^2 + r_{OH}{}^2 + 4a_O r\cos(\phi) + r^2\cos^2(\phi)) \qquad (5)$$

where a_H, b_H, and c_H are the inertial coordinates of the water hydrogens, a_O is the a coordinate of the oxygen atom, and $r = r_{OH}\cos(\theta/2)$, where r_{OH} and θ are the two internal coordinates of the water subunit. The ϕ-dependent terms in eq 5 amount to 8.5 u Å^2, whereas the corresponding contribution to $I_c - I_b$ is ca. 0.5 u Å^2. Structural fits were performed with program STRFIT[39] which was written to deal specifically with hydrogen-bonded complexes,[40] and which allows internal structural coordinates to be fitted directly to moments of inertia, as outlined by Schwendeman.[41] The monomer geometries were assumed to remain unchanged on complex formation, and r_0(OH) = 0.9650 Å, θ_0(HOH) = 104.78°,[42] and r_0(HCl) = 1.2839 Å[43] were used. The known isotopic dependence of these quantities on deuteration has also been accounted for. The O···HCl hydrogen bond was assumed to be linear since in the ab initio results it did not deviate from linearity by more than 2°.

TABLE 6: Structural Parameters for $H_2O\cdots HCl$ Determined from Fitting the $(B + C)$ Rotational Constants Separately to the Eight HCl and to the Six DCl Isotopomers

	HCl		DCl	
	planar	nonplanar	planar	nonplanar
R_0(OCl)/Å	3.2111(17)	3.2273(3)	3.2066(2)	3.2264(3)
ϕ/deg		34.7(4)		36.5(3)
σ/u Å^2	0.77	0.050	0.79	0.024

The results of fitting the molecular structure of $H_2O\cdots HCl$ to moments of inertia derived from the $(B + C)$ rotational constants are reported in Table 6. It is quite clear on statistical grounds that the nonplanar model leads to a much better reproduction of the experimental data. There is very good agreement of the experimentally fitted effective ground state out-of-plane bending angle for HCl isotopomers, $\phi_0 = 34.7(4)°$, with $\phi = \cos^{-1}\langle\cos(\phi)\rangle_{00} = 35.2°$ from the double minimum function. The small increase in ϕ_0 and (now smaller) decrease in R_0(OCl) for the DCl isotopomers are consistent with changes expected to be brought on by the Ubbelohde effect, but it is

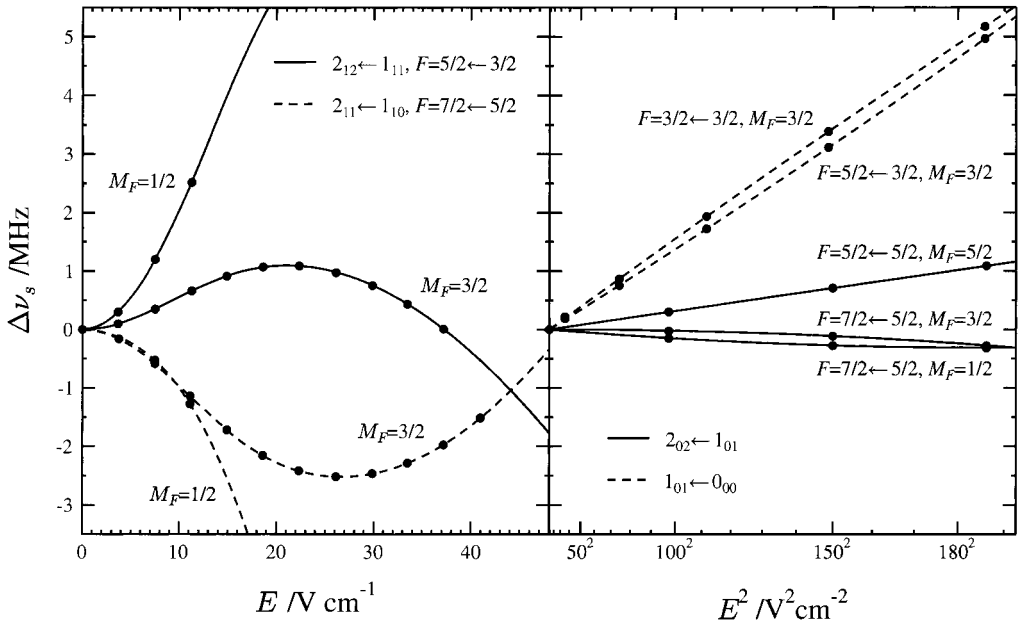

Figure 3. Electric field dependence of selected Stark components for $H_2O\cdots HCl$, the curves depict predictions from the full diagonalization treatment, the points are experimental measurements.

still not possible to analyze them quantitatively. It is noted that the use of the nonplanar model makes the ground-state heavy-atom distance longer than in the planar model, so that the previous value for R_0(OCl) of 3.215 Å[10] is presently revised to 3.227 Å. This value will still be subject to systematic error arising from the neglect of vibration−rotation contributions. On the basis of results for other complexes,[15,37,38] it can be estimated that harmonic vibration−rotation contributions to $I_b + I_c$ should not exceed 1 u Å^2. The average moment of inertia,[44] $(I_b + I_c)^*$, which is free from such contributions would then be limited by $(I_b + I_c)^* \leq (I_b + I_c)_0 + 1$, and the average structural quantities R^*(OCl) and ϕ^* would not exceed the ground-state ones by more than 0.006 Å and 0.5°, respectively.

Electric Dipole Moment

The separation of the Stark electrodes used to measure the dipole moment has to be kept sufficiently large so that the modes of the microwave resonator in the FTMW spectrometer are not perturbed. This leads to the use of relatively small electric fields and, as a consequence, the Stark splitting in the energy levels is comparable to the nuclear quadrupole splitting. For molecules containing quadrupolar nuclei, such as $H_2O\cdots HCl$, we thus find that it is necessary to work in the inconvenient intermediate field regime, for which simplified methods of Stark analysis lose their applicability. The only satisfactory solution is to set up and diagonalize the energy matrix separately for each value of the applied electric field. A fitting computer program, QSTARK, was written to deal with this problem.[39] The J, K_{-1}, K_{+1}, F, M_F quantization is used and the energy matrix is set up with irreducible tensor methods, with matrix elements for the nuclear quadrupole part of the Hamiltonian, H_Q, from ref 45, and for the electric field term, H_E, from ref 46. The success of the program can be assessed from the result that identical field calibrations are obtained on the basis of two different molecules, CH_3I and CH_3CN, both of which are subject to intermediate field effects.

The program was used to identify the most suitable Stark components for dipole moment measurement of $H_2O\cdots HCl$. A comparison of measurement and calculation for several selected Stark components is made in Figure 3. It can be seen that the majority of the $K_{-1} = 0$ components show some curvature in the E^2 representation, whereas in the $K_{-1} = 1$ components it is possible to observe avoided level crossing type behavior. All of these effects are satisfactorily fitted with a single value of the dipole moment, as summarized in Table 7. If there is any J or K_{-1} dependence of the dipole moment it is seen to be small, and μ_c cannot be determined with significance. The final value of the dipole moment for $H_2O\cdots HCl$, $\mu_{tot} = \mu_a = 3.437(4)$ D, carries a rather conservative error estimate, which encompasses all known uncertainties in the absolute calibration of the electric field.

A quantity of particular interest is the dipole moment enhancement on complex formation, $\Delta\mu$, which arises from additional polarization of electron density in the component molecules by their proximity. Table 8 compares experimental and theoretical results concerning this quantity for $H_2O\cdots HF$

TABLE 7: Experimental Dipole Moment of $H_2O\cdots HCl$

	N lines	σ/kHz	μ/D[a]
$K_{-1} = 0$: $1_{01} \leftarrow 0_{00}$	25	1.9	3.4367(3)
$K_{-1} = 0$: $2_{02} \leftarrow 1_{01}$	20	3.9	3.4424(32)
$K_{-1} = 1$: $2_{11} \leftarrow 1_{01}$, $2_{12} \leftarrow 1_{11}$	28	4.6	3.4353(13)
global fit	74	3.7	3.4365(5)
final value			$\mu = 3.437(4)$

[a] The cited error reflects the statistical uncertainty of the fit, apart from the lowest value which includes the uncertainty in the electric field calibration.

TABLE 8: Dipole Moment Enhancement (D) on Formation of the Complexes $H_2O\cdots HCl$ and $H_2O\cdots HF$

	$H_2O\cdots HF$		$H_2O\cdots HCl$	
	ab initio[a]	obs[b]	ab initio	obs
μ(HX)	1.811	1.826526(7)	1.181	1.1085(5)
$\mu(H_2O)$	1.877	1.85498(9)	1.877	1.85498(9)
$\mu_a(H_2O\cdots HX)$	4.195	4.073(7)	3.744	3.437(4)
$\Delta\mu$[c]	0.84	0.68	1.02	0.81

[a] The calculated values have been evaluated at the aug-cc-pVDZ/MP2 level, and are equilibrium values for the monomers and for the $\phi = \cos^{-1}\langle\cos(\phi)\rangle_{00}$ geometry for the dimers. [b] Ground-state values, HCl ref 47, HF ref 48, and H_2O ref 49. [c] The theoretical value is $\Delta\mu = \mu_a - \mu_{HX} - \mu_{H_2O}\cos\phi$, where μ_a is the a-axis component of the dipole moment calculated for $\phi = \cos^{-1}\langle\cos(\phi)\rangle_{00}$; the experimental value is $\Delta\mu^0 = \mu^0_{tot} - \mu^0_{HX} - \mu^0_{H_2O}\langle\cos(\phi)\rangle_{00}$.

TABLE 9: Comparison of Observed and Calculated Nuclear Quadrupole Splitting Constants (MHz) for HCl and $H_2O\cdots HCl$

		calculated				
	obs.	6-31G**	6-31G**/MP2	Sadlej/MP2[a]	aug-cc-pVDZ/MP2	aug-cc-pVTZ/MP2
$\chi(H^{35}Cl)$	−67.6189(5)[b]	−65.30	−64.64	−61.73	−57.92	−60.45
$\chi_{aa}(H_2O\cdots H^{35}Cl)$[c]		−55.23	−53.08	−51.80	−48.12	−51.18
$\chi_{aa}^{(sc)}(H_2O\cdots H^{35}Cl)$[d]	−53.414(3)	−57.2	−55.5	−56.8	−56.2	−57.4
η	0.0125(1)	0.0058	0.0053	0.0094	0.0091	0.0098

[a] Calculated at the aug-cc-pVDZ/MP2 geometry. [b] Ground-state value, ref 51. [c] Calculated from the field gradient by using $Q(^{35}Cl) = -0.0816$ barn, ref 52. [d] Scaled value, given by $\chi^{calc}(H_2O\cdots HCl)$ $[\chi^{obs}(HCl)/\chi^{calc}(HCl)]$, at each level of calculation.

and $H_2O\cdots HCl$. There are, however, several fine points, which first have to be considered. It is first necessary to keep in mind that the μ_c component of the dipole moment, perpendicular to the inversion plane, is averaged to zero by the inversion motion and is not experimentally measurable. Furthermore, although for a nonplanar equilibrium structure the μ_a component of the dipole moment will be approximately given by

$$\mu_a = \mu_{HCl} + \mu_{H_2O}\cos(\phi) + \Delta\mu \tag{6}$$

the corresponding relationship for the vibrational ground state will be[5]

$$\mu_{tot}^0 = \mu_a^0 = \mu_{HCl}^0 + \mu_{H_2O}^0\langle\cos(\phi)\rangle_{00} + \Delta\mu^0 \tag{7}$$

The experimental values of $\Delta\mu$ in Table 8 have been obtained by using eq 6. In order to make a meaningful comparison with the theoretical result it was necessary to decide on the quantity to use on the left-hand side of eq 6. The ab initio global minimum values, $\mu_a = 3.445$ D for $H_2O\cdots HCl$ and $\mu_a = 3.896$ D for $H_2O\cdots HF$ are not directly applicable since they are for values of ϕ, which are ca. 10° larger than the out-of-plane bend angle in the vibrational ground state. The most appropriate choice appears to be to calculate the dipole moment for the angle $\phi_0 = \cos^{-1}\langle\cos(\phi)\rangle_{00}$ i.e., 35.2° for $H_2O\cdots HCl$ and 36.7° for $H_2O\cdots HF$, and this is the prescription used for the theoretical values in Table 8. The comparison of theory and experiment is satisfactory for absolute values and accounts for all the trends. The difference between the experiment and calculation will be even smaller if the decrease in the effective ground-state value of the dipole moment of HCl in the dimer, μ_{HCl}^0 in eq 7, is taken into account. This quantity will be given by $\mu(\text{free HCl})\langle\cos(\theta_{av})\rangle_{00}$, ref 50, but since we show below that the averaging angle, θ_{av}, is relatively small, the corresponding decrease in μ_{HCl}^0 is expected to be well below 0.05D.

The most notable final result is that, even though the total dipole moment for $H_2O\cdots HCl$ is smaller than that of $H_2O\cdots HF$, the dipole moment enhancement for $H_2O\cdots HCl$ is appreciably higher. Experiment and calculation are in agreement on this observation, which reflects the considerably greater polarizability of HCl. The magnitude of $\Delta\mu$ was also compared with the result of a simple calculation of induced dipole moments, $\mu_{ind} = \alpha F_z$, from isotropic polarizabilities, α, of the two constituent molecules and fields, F_z, subtended by each onto its partner (calculated at the aug-cc-pVDZ/MP2 level). The resulting value, $\Delta\mu = 0.72$ D, is comparable to the values in Table 8 and breaks down into a 35% contribution from μ_{ind} on HCl due to the field of H_2O, and 65% from μ_{ind} on H_2O due to the field of HCl. This is a consequence of the field produced by HCl on H_2O being 3 times the field produced by H_2O on HCl, which outweighs the fact that the polarizability of HCl is twice that of H_2O.

Nuclear Quadrupole Coupling

The nuclear quadrupole coupling constant for the chlorine nucleus in $H_2O\cdots H^{35}Cl$ has been obtained from electric-field gradient calculations at several levels of theory, as reported in Table 9, where the computational results are compared with experiment. Values of quadrupole coupling constants are notoriously difficult to obtain with high accuracy, as conventional Gaussian basis sets underestimate the significant core contribution to the electric-field gradient at the nucleus,[53] and the present results are not free from this deficiency. Substantial underestimation of the magnitude of the field gradient is evident in the calculations for the free $H^{35}Cl$ molecule, where no complications of averaging or choice of axes arise to obscure the comparison. However, the main interest in ab initio calculation of these quantities is not in the absolute values but in the analysis of the changes produced by formation of the complex. Owing to the localized nature of the error, basis sets of modest size can still be expected to be useful for this analysis. Thus, in Table 9, the variation in the largest principal component, $\chi_{zz} = \chi_{aa}$, for $H_2O\cdots H^{35}Cl$ across the set of calculations tracks the variation in the parallel component of χ for the free molecule, when calculated in the same way. The supermolecule calculations should therefore allow realistic estimation of the electronic-structure-based effects of formation of the complex.

In the usual model of a weakly bound complex as an association of monomers that retain their separate identities, the difference between $\chi_{zz}(^{35}Cl)$ for the complex and the free HCl molecule is interpreted as a convolution of four effects. The electric-field gradient at Cl in the complex at equilibrium geometry differs from that in the free molecule (i) trivially by virtue of the different orientation of the principal axes of inertia, and (ii) because of the slight elongation of the HCl bond in the complex, but also (iii) because of the electrical perturbation of HCl by the nearby H_2O partner; this modified field gradient is then subject (iv) to angular averaging over the large-amplitude motion of the HCl subunit within the complex.

The electrical effect (iii) may be broken down into two parts: the "bare field-gradient" part of the nonuniform field of H_2O, and the response of the HCl electron cloud to this perturbation. The latter may be treated by a generalization of the theory of Sternheimer shieldings,[54−56] and in fact is the dominant factor in complexation shifts for attachment of HCl to polar monomers.

All but the vibrational averaging effect (iv) are present in a clamped-nucleus supermolecule calculation, and so comparison of the ab initio and experimental results in Table 9 should allow separation of equilibrium and motional averaging effects. Further decomposition of the equilibrium effects (i) to (ii) requires some subsidiary calculations.

Calculation of the field gradient in a free HCl molecule with nuclei placed at the principal-axis positions for the optimized complex takes account of effects (i) and (ii). In the 6-31G** basis, the combined effect of rotation and stretching of HCl is

to increase the magnitude of the calculated χ_{zz} (^{35}Cl), which becomes −66.9 MHz, and to introduce a small *xy* anisotropy of −0.02 MHz.

In the same basis, the bare field gradient at the chlorine position arising from the H_2O moiety is small: it has components 0.0246 (*xx*), −0.0092 (*yy*), and 0.0012 (*xy*), all in au, which are equivalent to contributions of only 0.47, −0.18, and 0.02 MHz to $\chi(^{35}Cl)$. The water monomer also produces a field at the chlorine site of (in au) 0.038 (*x*), −0.002 (*y*).

This relatively small perturbation is dramatically amplified by the response of the HCl electron cloud. A simple single-origin treatment in which the field and field gradient at the chlorine site are taken as uniform and added as finite perturbations to the SCF Hamiltonian produces a decrease in magnitude of ∼8 MHz in $\chi_{zz}(^{35}Cl)$. With more sophisticated representation of the highly nonuniform perturbing field,[56] even larger effects could be expected, but this simple model is already enough to show that most of the ∼10 MHz equilibrium shift in χ_{zz} found across the various calculations is a consequence of inductive polarization of HCl within the complex. Similar results are found in the larger bases.

The ab initio supermolecule results can be used to estimate the residual effect (iv) of motional averaging by scaling with the ratio of experimental and calculated coupling constants for free HCl. This should remove the major part of the absolute error in the calculated shifts and gives a reasonably consistent set of values for χ_{zz} in the dimer (Table 9). The results for the three largest bases suggest a reduction in magnitude of χ_{zz} by ∼3−4 MHz due to motional averaging, and imply an operationally defined oscillation angle θ_{av} of about 10−12°, rather than the angle of ∼22° (Table 4) that would be deduced by ignoring the electrical perturbation. The complex is thus considerably more rigid than the raw coupling constants might suggest. Similar discussion based on the deuterium quadrupole constant is at present precluded by the low accuracy of the pertinent experimental value. The present result concerning θ_{av} is consistent with that obtained for $H_2O\cdots HBr$,[57] for which correction for the response of HBr to presence of the H_2O subunit resulted in a net large-amplitude oscillation angle of 12.7°.

Conclusions

The extended isotopic measurements for $H_2O\cdots HCl$ and their analysis allowed the values of all spectroscopic observables in this complex to be well understood in terms of the molecular properties of the dimer. In particular, the ground-state molecular geometry has been determined with greater confidence than has been possible hitherto.[10] The effective geometry reflected by the moments of inertia is sensitive to the value of the quantum average $\langle\cos(\phi)\rangle_{00}$ and experimental data and the calculated double minimum function are in excellent quantitative agreement on the value of the angle $\phi_0 = \cos^{-1}\langle\cos(\phi)\rangle_{00}$. Both approaches establish that in the vibrational ground state the $H_2O\cdots HCl$ dimer is nonplanar, with the water unit bent by $\phi_0 \cong 35°$ away from the planar C_{2v} geometry. This is a consequence of the existence of two equivalent pyramidal equilibrium geometries, for $\phi = 46°$, separated by a potential barrier of 80 cm^{-1}.

Two useful ways of dealing with the spectroscopic data have been identified. It was found that fitting the $(B + C)$ rotational constant provides a robust method of deriving structural parameters for a prolate, near-planar complex since the effect of the vibration−rotation contributions on the derived parameters is minimized. In addition, approximation of the one-dimensional ab initio double minimum potential section with the spectroscopic quartic−quadratic potential function was found to be rather accurate so that this well understood analytical potential could be used as a useful shortcut for determining spectroscopic constants sensitive to the shape of the double minimum potential. Tests of these procedures for other $H_2O\cdots RX$ type dimers gave encouraging results and further work on understanding dimer geometry in the low-barrier case is in progress.

Acknowledgment. We are grateful to Dr M.J.Nowak for the sample of $H_2{}^{18}O$. Financing from the grant KBN-3T09A-126-17, the KBN/British Council Joint Research Collaboration Programme, and the Institute of Physics is acknowledged.

Supporting Information Available: Tables IS−IIIS of measured transitions frequency, and Table IVS of measured Stark components. This information is available free of charge via the Internet at http://pubs.acs.org.

References and Notes

(1) Legon, A. C.; Millen, D. J. *Faraday Discuss. Chem. Soc.* **1982**, *73*, 71.
(2) Georgiou, A. S.; Legon, A. C.; Millen, D. J. *Proc. R. Soc. London A* **1980**, *373*, 511.
(3) Georgiou, A. S.; Legon, A. C.; Millen, D. J. *J. Mol. Struct.* **1980**, *69*, 69.
(4) (a) Bevan, J. W.; Legon, A. C.; Millen, D. J.; Rogers, S. C. *J. Chem. Soc., Chem. Commun.* **1975**, 341. (b) Bevan, J. W.; Kisiel, Z.; Legon, A. C.; Millen, D. J.; Rogers, S. C. *Proc. R. Soc. London A* **1980**, *372*, 441.
(5) Kisiel, Z.; Legon, A. C.; Millen, D. J. *Proc. R. Soc. London A* **1982**, *381*, 419.
(6) Thomas, R. K. *Proc. R. Soc. London. A* **1975**, *344*, 579.
(7) Legon, A. C.; Millen, D. J.; North, H. M. *Chem. Phys. Lett.* **1987**, *135*, 303.
(8) Adebayo, S. L.;. Legon, A. C.;. Millen, D. J. *J. Chem. Soc., Faraday Trans.* **1991**, *87*, 443.
(9) Cazzoli, G.; Lister, D. G.; Legon, A. C.; Millen, D. J.; Kisiel, Z. *Chem. Phys. Lett.* **1985**, *117*, 543.
(10) Legon, A. C.; Willoughby, L. C. *Chem. Phys. Lett.* **1983**, *95*, 449.
(11) Kisiel, Z.; Kosarzewski, J.; Pszczółkowski, L. *Acta Phys. Pol. A* **1997**, *92*, 507.
(12) Kisiel, Z.; Pszczółkowski, L. *Chem. Phys. Lett.* **1998**, *291*, 190.
(13) Balle, T. J.; Flygare, W. H. *Rev. Sci. Instrum.* **1981**, *52*, 33.
(14) Kisiel, Z.; Białkowska-Jaworska, E.; Nowak, M. J.; Pszczółkowski, L., to be published.
(15) Kisiel, Z.; Białkowska-Jaworska, E.; Pszczółkowski, L.; Milet, A.; Struniewicz, C.; Moszynski, R.; Sadlej, J. *J. Chem. Phys.* **2000**, *112*, 5767.
(16) Gadhi, J.; Wlodarczak, G.; Legrand, J.; Demaison, J. *Chem. Phys. Lett.* **1989**, *156*, 401.
(17) Gadhi, J.; Lahrouni, A.; Legrand, J.; Demaison, J. *J. Chim. Phys. PCB* **1995**, *92*, 1984.
(18) Hepp, M.; Winnewisser, G.; Yamada, K. M. T. *J. Mol. Spectrosc.* **1991**, *146*, 181.
(19) Read, W. G.; Flygare, W. H. *J. Chem. Phys.* **1982**, *76*, 2238.
(20) Hellwege, K.-H., Ed. *Landolt Bornstein Numerical Data and Functional Relationships in Science and Technology*; Springer: Berlin, 1974; Vol. II/6.
(21) Novick, S. E.; Davies, P.; Harris, S. J.; Klemperer, W. *J. Chem. Phys.* **1973**, *59*, 2273.
(22) Read, W. G.; Campbell, E. J.; Henderson, G. J. *J. Chem. Phys.* **1983**, *95*, 3501.
(23) Millen, D. J. *Can. J. Chem.* **1985**, *63*, 1477.
(24) Ubbelohde, A. R.; Gallagher, K. J. *Acta Crystallogr.* **1955**, *8*, 71.
(25) Kisiel, Z.; Legon, A. C.; Millen, D. J. *J. Mol. Struct.* **1984**, *112*, 1.
(26) Schmidt, M. W.; Baldridge, K. K.; Boatz, J. A.; Elbert, S. T.; Gordon, M. S.; Jensen, J. H.; Koseki, S.; Matsunaga, N.; Nguyen, K. A.;.Su, S. J.; Windus, T. L.; Dupuis, M.; Montgomery, J. A. *J. Comput. Chem.* **1993**, *14*, 1347.
(27) (a) Dunning, T. H., Jr. *J. Chem. Phys.* **1989**, *90*, 1007. (b) Kendall, R. A.; Dunning, T. H., Jr.; Harrison, R. J. *J. Chem. Phys.* **1992**, *96*, 6769.
(28) Xantheas, S. S.; Dunning, T. H. *J. Chem. Phys.* **1993**, *99*, 8774.
(29) Xantheas, S. S. *J. Chem. Phys.* **1994**, *100*, 7523.
(30) Boys, S. F.; Bernardi, F. *Mol. Phys.* **1970**, *4*, 553.
(31) Latajka, Z.; Scheiner, S. *J. Chem. Phys.* **1987**, *87*, 5928.
(32) Packer, M. J.; Clary, D. C. *J. Phys. Chem.* **1995**, *99*, 14323.
(33) Laane, J. *Appl. Spectrosc.* **1970**, *24*, 73.
(34) Kisiel, Z. Ph.D. Thesis, University of London, 1980.
(35) Kraitchman, J. *Am. J. Phys.* **1953**, *21*, 17.

(36) Costain, C. C. *Trans. Am. Crystallogr. Assoc.* **1966**, *2* 157.
(37) Kisiel, Z.; Fowler, P. W.; Legon, A. C. *J. Chem. Phys.* **1994**, *101*, 4635.
(38) Kisiel, Z.; Fowler, P. W.; Legon, A. C. *J. Chem. Soc., Faraday Trans.* **1992**, *88*, 3385.
(39) Kisiel, Z. *PROSPE—Programs for Rotational Spectroscopy* database, http://info.ifpan.edu.pl/~kisiel/prospe.htm.
(40) Kisiel, Z.; Fowler, P. W.; Legon, A. C. *J. Chem. Phys.* **1990**, *93*, 3062.
(41) Schwendeman, R. H. In *Critical Evaluation of Chemical and Physical Structural Information*; Lide, D. R., Paul, M. A., Eds.; National Academy of Sciences: Washington, DC, 1974.
(42) DeLucia, F. C.; Helminger, P.; Cook, R. L.; Gordy, W. *Phys. Rev. A* **1972**, *5*, 487.
(43) DeLucia, F. C.; Helminger, P.; Gordy, W. *Phys. Rev. A* **1971**, *3*, 1849.
(44) Gordy, W.; Cook, R. L. *Microwave Molecular Spectra*; John Wiley and Sons: New York, 1984; Chapter XIII.
(45) (a) Keenan, M. R.; Wozniak, D. B.; Flygare, W. H. *J. Chem. Phys* **1981**, *75*, 631. (b) Read, W. G.; Flygare, W. H. *J. Chem. Phys.* **1982**, *76*, 2238.
(46) Benz, H. P.; Bauder, A.; Gunthard, Hs. H. *J. Mol. Spectrosc.* **1966**, *21*, 156.
(47) Kaiser, E. W. *J. Chem. Phys.* **1970**, *53*, 1686.
(48) Muenter, J. S.; Klemperer, W. *J. Chem. Phys.* **1970**, *52*, 6033.
(49) Shostak, S. L.; Ebenstein, W. L.; Muenter, J. S. *J. Chem. Phys.* **1991**, *94*, 5875.
(50) Hutson, J. M. *J. Chem. Phys.* **1988**, *89*, 4550.
(51) Kaiser, E. W. *J. Chem. Phys.* **1970**, *53*, 1686.
(52) Kellö, V.; Sadlej, J. *Mol. Phys.* **1996**, *89*, 27.
(53) Halkier, A.; Jaszunski, M.; Jorgensen, P. *Phys. Chem. Chem. Phys.* **1999**, *1*, 4165.
(54) Fowler, P. W.; Lazzeretti, P.; Steiner, E.; Zanasi, R. *Chem. Phys.* **1989**, *133*, 221.
(55) Baker, J.; Buckingham, A. D.; Fowler, P. W.; Lazzeretti, P.; Steiner, E.; Zanasi, R. *J. Chem. Soc., Faraday Trans. 2* **1989**, *85*, 901.
(56) Buckingham, A. D.; Fowler, P. W.; Legon, A. C.; Peebles, S. A.; Steiner, E. *Chem. Phys. Lett.* **1995**, *232*, 437.
(57) Legon, A. C.; Suckley, A. P. *Chem. Phys. Lett.* **1988**, *150*, 153.